Diffusion of a sphere in a dilute solution of polymer coils

Matthias Krüger[1,a)] and Markus Rauscher[2]

[1]Fachbereich Physik, Universität Konstanz, 78467 Konstanz, Germany
[2]Max-Planck-Institut für Metallforschung, Heisenbergstr. 3, 70569 Stuttgart, Germany and Institut für Theoretische und Angewandte Physik, Universität Stuttgart, Pfaffenwaldring 57, 70569 Stuttgart, Germany

We calculate the short time and the long time diffusion coefficients of a spherical tracer particle in a polymer solution in the low density limit by solving the Smoluchowski equation for a two-particle system and applying a generalized Einstein relation (fluctuation dissipation theorem). The tracer particle as well as the polymer coils are idealized as hard spheres with a no-slip boundary condition for the solvent but the hydrodynamic radius of the polymer coils is allowed to be smaller than the direct-interaction radius. We take hydrodynamic interactions up to 11th order in the particle distance into account. For the limit of small polymers, the expected generalized Stokes–Einstein relation is found. The long time diffusion coefficient also roughly obeys the generalized Stokes–Einstein relation for larger polymers whereas the short time coefficient does not. We find good qualitative and quantitative agreement to experiments.

I. INTRODUCTION

Transport properties of Brownian particles in suspensions are of great interest for all technological applications involving complex fluids such as food technology or oil recovery and they have been studied extensively experimentally (see, e.g., Refs. 1 and 2) and theoretically (see, e.g., Refs. 3–7). The diffusion constant D_s of a spherical tracer particle with radius R_s in a simple solvent is to a good approximation given by the Stokes–Einstein relation

$$D_s = \frac{k_B T}{6\pi R_s \eta_0},\qquad(1)$$

with the solvent viscosity η_0 and the thermal energy $k_B T$. As demonstrated, e.g., for the case of a tracer sphere in solution of polymers,[8–11] the naive approach to replace the pure solvent viscosity with the macroscopic shear viscosity η_{macro} of the polymer solution (as measured in a viscosimeter) in general fails. The polymer solution in the vicinity of the moving sphere is not homogeneous. Even in equilibrium one observes depletion layers or density oscillations (depending on the interaction potentials between the polymers and between the polymer and the particle). In the vicinity of a moving particle, the flowing solvent rearranges the polymers leading to an enhanced polymer density in front and a reduced polymer density behind the particle,[12] which leads to an enhanced friction,[13–15] and to long-ranged solvent mediated effective interactions.[16,17] The time scale for the buildup of these inhomogeneities in the solution in the vicinity of the moving particle is given by the diffusivity of the polymers and the particle size. For most systems this time scale is well separated from the corresponding microscopic time scale of the solvent,[18–20] but rather close to the time scale of the particle

diffusion (given by the particle size and its diffusion constant in the pure solvent).

For such systems, the mean square displacement is not linear in time and for the tracer particle one defines a time dependent diffusion coefficient $D_s(t)$ via[21]

$$D_s(t)t = \frac{1}{6}\langle(\mathbf{r}_s(t) - \mathbf{r}_s(t=0))^2\rangle,\qquad(2)$$

with the particle position $\mathbf{r}_s(t)$ at time t. $\langle\cdot\rangle$ indicates the equilibrium ensemble average. The short and the long time limits of $D_s(t)$ are called the short and long time diffusion coefficients

$$D_s^s = \lim_{t\to 0} D_s(t)\qquad(3)$$

and

$$D_s^l = \lim_{t\to\infty} D_s(t),\qquad(4)$$

respectively. The diffusion coefficient $D_s(t)$ is related to the time-dependent mobility coefficient $\mu_s(t)$ via the fluctuation-dissipation theorem, i.e., the generalized Einstein relation

$$\mu_s(t) = \beta \frac{\partial}{\partial t}[D_s(t)t],\qquad(5)$$

with $\beta = 1/(k_B T)$. $\mu_s(t)$ is the linear response mobility defined by the ratio of the average velocity of the particle and a small and constant external force $\mathbf{F}^{\text{ext}}$ that starts to act on the particle at $t=0$. Therefore, at time $t=0$, the distribution of polymers around the sphere is still in equilibrium, and the short time mobility $\mu_s^s = \lim_{t\to 0} \mu_s(t) = \beta D_s^s$ is solely determined by the hydrodynamic forces on the tracer. Once the sphere is in motion, the distribution of polymers in the vicinity of the tracer becomes anisotropic: it is more likely to find a polymer in front of the sphere than behind it, which reduces the mobility of the sphere. After a sufficiently long time, the polymer distribution becomes stationary and the velocity is
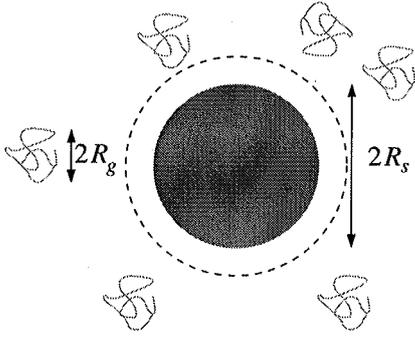
FIG. 1. A tracer sphere with radius R_s is suspended in a dilute solution of polymer coils with radii of gyration R_g. In a model with hard-sphere interactions, the centers of mass of the polymer coils cannot pass the dashed surface with radius $R = R_g + R_s$.

related to the force via the long time mobility coefficient $\mu_s^l = \lim_{t \to \infty} \mu_s(t) = \beta D_s^l$. In general $\mu_s^l \le \mu_s^s$.

Most of the theoretical work focuses on the semidilute regime with effective or mean field models,[22–25] see Ref. 26 for a summary. The depletion of polymers near the surface of the colloid was considered in Ref. 27. Recently, a model based on the reduced viscosity of the polymer solution near the colloid due to depletion was introduced.[28,29] However, up to now, the distinction between short and long time diffusion coefficients has been considered only for suspensions of hard spheres.[5,30–33] One main distinction between hard spheres and polymers is that for hard spheres the hydrodynamic radius is equal to the particle radius, while for polymers, the effective hydrodynamic radius is in general smaller than the radius of gyration. A different hydrodynamic and sphere radius has been used as a model for charged colloids,[34] but only the case of equal tracer and bath particles was considered. In this paper, we focus on the regime of a dilute polymer solution but we distinguish between the short and long time diffusivities. We idealize the tracer particle and the polymer coils as hard spheres concerning both the direct and hydrodynamic interactions, but with a hydrodynamic radius which can be smaller than the interaction radius in the case of the polymers.

In Sec. II, we present our model system and in Sec. III we calculate the short and long time diffusion coefficients from the corresponding Smoluchowski (or Fokker–Planck) equation. The results are compared to experimental values in Sec. V and we conclude in Sec. VI.

II. MODEL

We model the tracer particle as well as the polymer coils as spherical overdamped Brownian particles with radii R_s and R_g, respectively, as shown in Fig. 1. The bare diffusion coefficients of the sphere and the polymers in the pure solvent are D_s^0 and D_p (indices s and p will denote the sphere and the polymer, respectively, throughout the paper), respectively, which are calculated via the Stokes–Einstein relation in the pure solvent with viscosity η_0. The hydrodynamic radius which enters the Stokes–Einstein relation is equal to R_s
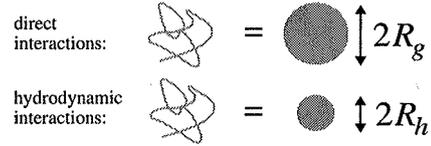

FIG. 2. We model the polymer coils as hard spheres of radius R_g concerning the interactions with the tracer sphere and as solid sphere of radius R_h and a no-slip boundary condition on the surface concerning the interactions with the solvent.

for the tracer and $R_h \le R_g$ for the polymers, see Fig. 2. We idealize the direct interaction between the tracer and the polymers as a hard-sphere interaction

$$V(r) = \begin{cases} 0 & \text{for} \quad r > R_s + R_g \\ \infty & \text{for} \quad r < R_s + R_g \end{cases} . \tag{6}$$

$r = |\mathbf{r}| = |\mathbf{r}_s - \mathbf{r}_p|$ denotes the distance of the centers of the tracer and a polymer. As a consequence, the center of mass of the polymers can approach the center of the tracer only up to a distance $R = R_s + R_g$. In the dilute limit, we neglect the mutual interactions of the polymer particles, which reduces the problem effectively to a two-particle system of one tracer sphere and one polymer coil.

The dynamics of the system is described by the Smoluchowski equation for the probability density $P(\mathbf{r}_s, \mathbf{r}_p)$ for finding the tracer sphere at position $\mathbf{r}_s$ and the polymer coil at $\mathbf{r}_p$. The Smoluchowski equation is a continuity equation and with the corresponding probability currents $\mathbf{j}_{s/p}$ we can define the velocity operators such that $\mathbf{j}_{s/p} = \mathbf{v}_{s/p} P$,

$$\frac{\partial}{\partial t} P = - \begin{pmatrix} \mathbf{\nabla}_s \\ \mathbf{\nabla}_p \end{pmatrix} \cdot \begin{pmatrix} \mathbf{j}_s \\ \mathbf{j}_p \end{pmatrix}$$

$$= - \begin{pmatrix} \mathbf{\nabla}_s \\ \mathbf{\nabla}_p \end{pmatrix} \cdot \begin{pmatrix} \mathbf{v}_s P \\ \mathbf{v}_p P \end{pmatrix}$$

$$= \begin{pmatrix} \mathbf{\nabla}_s \\ \mathbf{\nabla}_p \end{pmatrix} \cdot \left[\mathbf{D} \cdot \begin{pmatrix} \beta[\mathbf{\nabla}_s V] - \beta \mathbf{F}^{\text{ext}} + \mathbf{\nabla}_s \\ \beta[\mathbf{\nabla}_p V] + \mathbf{\nabla}_p \end{pmatrix} P \right], \tag{7}$$

with the external force $\mathbf{F}^{\text{ext}}$. $\mathbf{\nabla}_s$ and $\mathbf{\nabla}_p$ denote the gradient with respect to the position of the sphere and the polymer, respectively. The components of the symmetric diffusivity matrix

$$\mathbf{D} = \begin{pmatrix} \mathbf{D}_{ss} & \mathbf{D}_{ps} \\ \mathbf{D}_{sp} & \mathbf{D}_{pp} \end{pmatrix} \tag{8}$$

have the form

$$\mathbf{D}_{ss} = D_s^0 [D_{ss}^r(r) \mathbf{P} + D_{ss}^\theta(r)(1 - \mathbf{P})], \tag{9a}$$

$$\mathbf{D}_{pp} = D_p [D_{pp}^r(r) \mathbf{P} + D_{pp}^\theta(r)(1 - \mathbf{P})], \tag{9b}$$

$$\mathbf{D}_{sp} = \mathbf{D}_{sp} = D_s^0 [D_{sp}^r(r) \mathbf{P} + D_{sp}^\theta(r)(1 - \mathbf{P})]. \tag{9c}$$

The projector $\mathbf{P}$ is given by $\hat{\mathbf{r}} \hat{\mathbf{r}}$ with $\hat{\mathbf{r}} = \mathbf{r}/r$. The r-dependent coefficients D_{ss}^r, D_{ss}^θ, D_{pp}^r, D_{pp}^θ, D_{ps}^r, and D_{ps}^θ can be expanded in a power series in r^{-1}. We use the coefficients for spheres with no-slip hydrodynamic boundary conditions on their surfaces up to order r^{-11} in the distance according to Ref. 35. We quote the coefficients for two unequal spheres of radii R_s

and R_h for the tracer and the polymer, respectively, in the Appendix. We therefore assume that the polymer interacts with the solvent like a solid sphere with radius R_h, see Fig. 2. For the case of hard-sphere suspensions, also lubrication forces have been taken into account.[5] In the case considered here, the radius of gyration R_g is always larger than R_h, i.e., the hydrodynamically interacting spheres never come into contact and the far field expansion converges well. The diffusion matrices (9) are valid on the Brownian time scale and for small Reynolds numbers.[21]

Equation (7) is translationally invariant since $\mathbf{D}$ depends only on $\mathbf{r}=\mathbf{r}_s-\mathbf{r}_p$. As a consequence, P is a function of $\mathbf{r}$ only, and the hard interaction potential V in Eq. (6) can be translated into a no-flux boundary condition on a sphere of radius R,

$$\hat{\mathbf{r}} \cdot (\mathbf{j}_s - \mathbf{j}_p) = 0 \quad \text{at } |\mathbf{r}| = R. \tag{10}$$

In thermal equilibrium (for which $\mathbf{F}^{\text{ext}}=0$ is a necessary condition) detailed balance holds and all components of the probability currents $\mathbf{j}_{s/p}$ are zero. The equilibrium distribution and therefore also the initial condition for the dynamical problem equation (7) are therefore given by

$$P(\mathbf{r},t) = P^{\text{eq}}(\mathbf{r}) = \rho\Theta(|\mathbf{r}| - R) \quad \text{at } t = 0, \tag{11}$$

with the average number density of polymer molecules ρ. Far from the tracer sphere, the polymer distribution should be unaffected by the presence of the sphere and therefore equal to the corresponding equilibrium distribution, which yields the boundary condition

$$P(\mathbf{r},t) \to P^{\text{eq}}(\mathbf{r}) = \rho \quad \text{for } |\mathbf{r}| \to \infty. \tag{12}$$

In the linear response regime, the average velocity of the tracer particle is given by [$\langle \cdot \rangle^F(t)$ denotes the time dependent nonequilibrium average]

$$\langle \mathbf{v}_s \rangle^F(t) = \int \mathbf{j}_s(\mathbf{r},t)d^3r = \int \mathbf{v}_s P(\mathbf{r},t)d^3r = \mu_s(t)\mathbf{F}^{\text{ext}}, \tag{13}$$

such that we can calculate the short and long term diffusion coefficients from the solution of the Smoluchowski equation (7): once $P(\mathbf{r},t)$ is known, Eq. (13) yields the mobility coefficient $\mu_s(t)$, from which we calculate the diffusion coefficients through the generalized Einstein relation equation (5). Since $D_s(t)$ has to be finite for $t \to 0$, the integration constant which appears when solving Eq. (5) for D_s has to be zero.

Inserting the expression for $\mathbf{v}_s P$ from Eq. (7) into Eq. (13) we can decompose the velocity into three components,

$$\langle \mathbf{v}_s \rangle^F(t) = \beta\langle \mathbf{D}_{ss} \rangle \cdot \mathbf{F}^{\text{ext}} + \langle \mathbf{v}_s^I \rangle^F(t) + \langle \mathbf{v}_s^{\text{Br}} \rangle^F(t), \tag{14}$$

with

$$\langle \mathbf{v}_s^I \rangle^F(t) = - \beta\langle \mathbf{D}_{ss} \cdot \nabla V - \mathbf{D}_{sp} \cdot \nabla V \rangle^F(t), \tag{15}$$

$$\langle \mathbf{v}_s^{\text{Br}} \rangle^F(t) = - \beta\langle \mathbf{D}_{ss} \cdot \nabla \ln P - \mathbf{D}_{sp} \cdot \nabla \ln P \rangle^F(t). \tag{16}$$

Since P only depends on $\mathbf{r}=\mathbf{r}_s-\mathbf{r}_p$, we have replaced the gradients with respect to the positions of the tracer and the polymer with $\nabla=\nabla_s=-\nabla_p$. $\mathbf{v}_s^I$ and $\mathbf{v}_s^{\text{Br}}$ are the result of the direct interactions and the Brownian force, respectively.[21]

In the short time limit, i.e., at $t=0$, $P(\mathbf{r},t)$ is given by the initial condition, i.e., by $P^{\text{eq}}(\mathbf{r})$. By symmetry, both $\langle \mathbf{v}_s^I \rangle$ and $\langle \mathbf{v}_s^{\text{Br}} \rangle$ are zero in this limit.

In the long time limit $P(\mathbf{r},t)$ reaches a steady state $P(\mathbf{r},t) \to P^{\infty}(\mathbf{r})$ for $t \to \infty$, which is given by the solution of the stationary version of Eq. (7) (for $r>R$),

$$0 = \nabla \cdot (\mathbf{D}_{ss} + \mathbf{D}_{pp}) \cdot \nabla P^{\infty} - \nabla \cdot \mathbf{D}_{ss} \cdot \beta P^{\infty}\mathbf{F}^{\text{ext}}$$
$$- \nabla \cdot [\mathbf{D}_{sp} \cdot \{2 \nabla P^{\infty} - \beta P^{\infty}\mathbf{F}^{\text{ext}}\}]. \tag{17}$$

Since we are interested in the linear response regime, we expand $P^{\infty}(\mathbf{r})$ in powers of $\mathbf{F}^{\text{ext}}$ up to linear order, i.e., we seek a solution of the form[21]

$$P^{\infty}(\mathbf{r}) = P^{\text{eq}}(\mathbf{r})[1 + \beta A(r)\hat{\mathbf{r}} \cdot \mathbf{F}^{\text{ext}}]. \tag{18}$$

Inserting Eq. (18) into Eq. (17) and keeping only terms linear in $\mathbf{F}^{\text{ext}}$ yields a second order linear differential equation for the coefficient $A(r)$. Since we expand the mobility matrix $\mathbf{D}(r)$ in Eq. (7) in a power series in $1/r$ up to order $O(r^{-11})$, we choose the following ansatz for $A(r)$:

$$A(r) = \sum_{l=1}^{11} \frac{c_l}{r^l}, \tag{19}$$

which turns this differential equation into an algebraic equation for the coefficients c_l. It can be solved for the $c_{l \neq 2}$ in terms of c_2. Note that $c_1=0$. c_2 finally is determined by the boundary condition (10) at short distances, which reads in terms of $A(r)$,

$$\left. \frac{dA(r)}{dr} \right|_{r=R} = \frac{D_{ss}^r(R) - D_{sp}^r(R)}{D_{ss}^r(R) + \frac{D_p}{D_s^0}D_{pp}^r(R) - 2D_{sp}^r(R)}. \tag{20}$$

We solve the above equations using the computer algebra system MATHEMATICA.

III. SHORT AND LONG TIME DIFFUSION COEFFICIENTS

In the following we evaluate the three contributions to the average velocity of the sphere, i.e., $\beta\langle \mathbf{D}_{ss} \rangle \cdot \mathbf{F}^{\text{ext}}$, $\langle \mathbf{v}_s^I \rangle^F$, and $\langle \mathbf{v}_s^{\text{Br}} \rangle^F$ from Eq. (14) with $\langle \cdot \rangle^F \equiv \langle \cdot \rangle^F(t \to \infty)$. Since $\langle \mathbf{D}_{ss} \rangle$ is explicitly multiplied by $\mathbf{F}^{\text{ext}}$, in the linear response regime the coefficient $\mathbf{D}_{ss}$ in the first contribution has to be averaged with respect to the equilibrium distribution P^{eq} for all times t. Therefore the short time diffusion coefficient D_s^s of the sphere equals the first contribution to the long time diffusion coefficient

$$\frac{D_s^s}{D_s^0} = 1 + \frac{4\pi}{3}\rho\int_R^{\infty} dr\,r^2[(D_{ss}^r(r) - 1) + 2(D_{ss}^{\theta}(r) - 1)]$$

$$\equiv 1 - a_s\rho, \tag{21}$$

with

$$\frac{3a_s}{4\pi} = \frac{5R_h^3}{2} - \frac{5R_g R_h^3}{2R} + \frac{2R_h^5 + 5R_g^2 R_h^3}{R^2} + \frac{\dfrac{375R_h^6}{28} - 12R_g R_h^5 - 10R_g^3 R_h^3}{R^3} - \frac{609R_h^7 + 7500R_g R_h^6 - 4550R_g^2 R_h^5 - 875R_g^4 R_h^3}{140R^4}$$

$$- \frac{-2079R_g R_h^7 - 11250R_g^2 R_h^6 + 5600R_g^3 R_h^5 + 175R_g^5 R_h^3}{140R^5} - \frac{-36R_h^9 + 882R_g^2 R_h^7 + 3000R_g^3 R_h^6 - 1225R_g^4 R_h^5}{56R^6}$$

$$- \frac{36R_g R_h^9 - 294R_g^3 R_h^7 - 750R_g^4 R_h^6 + 245R_g^5 R_h^5}{56R^7}. \tag{22}$$

For evaluating the interaction velocity defined in Eq. (15) in the stationary limit, we note that the gradient of the potential V is only nonzero at $r=R$ and points in direction $\mathbf{r}$. This leads to

$$\langle \mathbf{v}_s^I \rangle^F = \beta D_s^0 \frac{4\pi}{3} R^2 A(R) [D_{ss}^r(R) - D_{sp}^r(R)] \mathbf{F}^{\text{ext}},$$

$$\equiv -a_I \beta D_s^0 \mathbf{F}^{\text{ext}}. \tag{23}$$

With a partial integration with respect to r the stationary Brownian velocity defined in Eq. (16) is given by

$$\langle \mathbf{v}_s^{\text{Br}} \rangle^F = \beta D_s^0 \frac{4\pi}{3} \rho \int_R^\infty dr A(r) \left[\frac{\partial}{\partial r} r^2 (D_{ss}^r(r) - D_{sp}^r(r)) \right.$$

$$\left. - 2r(D_{ss}^\theta(r) - D_{sp}^\theta(r)) \right] \mathbf{F}^{\text{ext}},$$

$$\equiv -a_{\text{Br}} \beta D_s^0 \mathbf{F}^{\text{ext}}. \tag{24}$$

Combining the three contributions, the long time diffusion coefficient of the sphere is finally given by

$$D_s^l = D_s^0 [1 - (a_s + a_I + a_{\text{Br}})\rho] \equiv D_s^0 (1 - a_I \rho). \tag{25}$$

Equations (21) and (25) can also be stated as functions of mass density c (which is often used in the experimental literature) of polymer coils rather than the number density ρ by using $c = \rho(M/N_A)$, with Avogadro's number N_A and the molecular mass of the polymer coils M. The coefficients a_s' and a_l' relating the mass density to the short and long time diffusion constants are then given by $a_s' = a_s(N_A/M)$ and $a_l' = a_l(N_A/M)$, respectively.

IV. RESULTS

The coefficients a_s and a_l for the short and long time coefficients are functions of R_s, R_g, and R_h and they can be written as the product of R_g^3 and a function that depends only on $\zeta = R_g/R_s$ and $\xi = R_g/R_h$. For hard spheres $\xi = 1$. For large polymers in good solvent conditions, ξ approaches a universal value of $\xi \approx 1.6$, see Ref. 36 and references therein. In order to be able to compare our results to the case of hard spheres,[5] we introduce the polymer packing fraction $\phi_p = (4\pi/3)R_g^3 \rho$ and define

$$a_{s/l}(R_s, R_g, R_h)\rho = \tilde{a}_{s/l}(\zeta, \xi)\phi_p. \tag{26}$$

Figure 3 shows $\tilde{a}_s(\zeta, \xi)$ and $\tilde{a}_l(\zeta, \xi)$ as function of ζ for different values of ξ between one and two.

For $\zeta \to 0$, i.e., for tracer particles large as compared to the polymer coils (this limit is often referred to as the colloid limit), the polymer solution as seen from the colloid behaves like a continuum, the probability distribution $P^\infty(r)$ approaches $P^{\text{eq}}(r)$, and both $\tilde{a}_s$ and $\tilde{a}_l$ converge to the continuum result

$$\lim_{\zeta \to 0} \tilde{a}_s = \lim_{\zeta \to 0} \tilde{a}_l = \frac{5}{2\xi^3}. \tag{27}$$

This leads to the generalized (sometimes also called effective) Stokes–Einstein relation for the diffusion coefficients

$$\lim_{\zeta \to 0} D_s^l = \lim_{\zeta \to 0} D_s^s = \frac{k_B T}{6\pi R_s \eta_\infty}, \tag{28}$$

with the Einstein result for the zero-shear high-frequency limiting viscosity of the polymer solution

$$\eta_\infty = \frac{\eta_0}{1 - \dfrac{5}{2}\dfrac{4\pi}{3}R_h^3 \rho} = \eta_0 \left(1 + \frac{5}{2}\frac{4\pi}{3}R_h^3 \rho \right) + \mathcal{O}(\rho^2). \tag{29}$$

η_0 is the Newtonian viscosity of the (polymer-free) solvent. Note that the next term in $\tilde{a}_{s/l}$ is of $\mathcal{O}(\zeta)$, while the difference between $\tilde{a}_s$ and $\tilde{a}_l$ is of $\mathcal{O}(\zeta^2)$.

For $\zeta \to \infty$, i.e., in the so-called protein limit in which the tracer particle is small as compared to the polymer coils, $\tilde{a}_s \to 0$ and the short time diffusion coefficient approaches the value in the pure solvent D_s^0 from below. The long time diffusion coefficient reaches a finite value which is smaller than D_s^0,

$$\lim_{\zeta \to \infty} \tilde{a}_l = \frac{1}{2}. \tag{30}$$

It is important to note that our model is limited to the case where the colloid does not enter the polymer, i.e., the colloid must remain larger than the "mesh size" of the polymer. In the protein limit, the diffusion coefficients are independent of hydrodynamic interactions since the small tracer does not perturb the solvent significantly. Both short and long time coefficients approach the value of the corresponding calculation neglecting hydrodynamic interactions. This simplifies Eq. (17) significantly and we get the analytic results
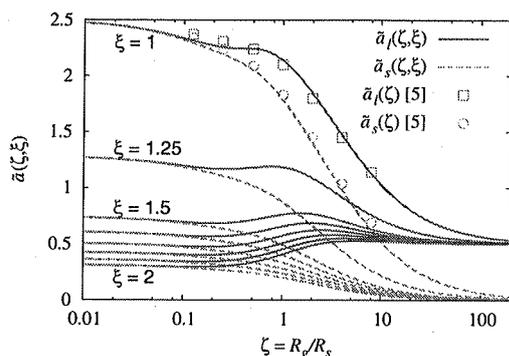
FIG. 3. $\tilde{a}_l$ and $\tilde{a}_s$ (solid blue and dashed red lines, respectively) defined via $D_s^{l/s}/D_s^0 = 1 - \tilde{a}_{l/s}\phi_p$ as functions of $\zeta = R_g/R_s$ for different values of the ratio $\xi = R_g/R_h$. The value of ξ for neighboring curves for the lowest six curves differs by 0.1. Squares and circles indicate the results for the long and short time diffusion constants of hard spheres ($\xi = 1$), respectively, according to Ref. 5.

$\tilde{a}_s^{(\text{noHI})} = 0$ and $\tilde{a}_l^{(\text{noHI})} = (1 + 1/\zeta)^3/(2 + 2\xi/\zeta)$, with $\tilde{a}_l^{(\text{noHI})} \rightarrow \frac{1}{2}$ for $\zeta \rightarrow \infty$.

For a very long polymer in good solvent conditions $\xi \approx 1.6$. The corresponding values of $\tilde{a}_l$ and $\tilde{a}_s$ as functions of ζ are shown in Fig. 4. In contrast to the short time coefficient $\tilde{a}_s$ which decreases monotonically as a function of ζ the long time coefficient $\tilde{a}_l(\zeta, \xi = 1.6)$ has a maximum at $\zeta \approx \xi$. That means for $R_h \lesssim R_s$ ($\zeta \lesssim \xi$), larger spheres are less hindered in their motion by the polymer coils than smaller spheres, while the situation is reverse for $R_h \gtrsim R_s$ ($\zeta \gtrsim \xi$). This is in agreement with experiments as demonstrated in Sec. V A. The variation in $\tilde{a}_l$ over all ζ is nevertheless rather weak (about $\pm 15\%$), which means that the generalized Stokes–Einstein relation is an acceptable approximation for all values of ζ. However, this is only the case for $\xi \approx 1.6$, for which the limits of $\tilde{a}_l$ for $\zeta \rightarrow 0$ and for $\zeta \rightarrow \infty$ are not too different. In contrast to the long time diffusion coefficient, the short time diffusion coefficient varies strongly as a function of ζ, such that the generalized Stokes–Einstein relation for $\tilde{a}_s$ holds only in the limit $\zeta \rightarrow 0$. The maximum of $\tilde{a}_l(\zeta, \xi = 1.6)$ at $\zeta = \xi$ is the result of two competing effects. With decreasing R_s (increasing ζ) the solvent flow field generated by the mov-
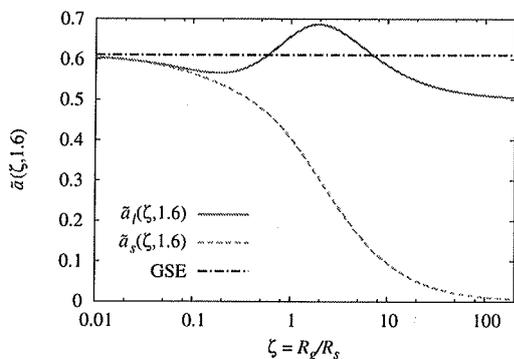

FIG. 4. $\tilde{a}_l$ and $\tilde{a}_s$ (solid blue and dashed red lines, respectively) for large polymers in good solvent conditions ($\xi = R_g/R_h = 1.6$) as function of ζ. Also shown is the result for the generalized Stokes–Einstein relation equation (28), which is independent of $\zeta = R_g/R_s$. In this approximation short and long time diffusion constants are equal.

ing tracer is weaker and as a consequence the short time diffusivity increases, i.e., $\tilde{a}_s$, and, according to Eq. (25), $\tilde{a}_l$ decrease. On the other hand, the distribution of bath particles around the tracer gets more disturbed since the weaker flow field cannot transport the bath particles around the tracer such that these accumulate in front of the tracer, which reduces the tracer mobility.[14,15] For very large ζ the decreasing short time coefficient $\tilde{a}_s$ dominates but at intermediate ζ the accumulation of bath particles leads to a local maximum of $\tilde{a}_l$. This mechanism only leads to a local maximum of $\tilde{a}_l$ for intermediate values of ξ.

The long time diffusion coefficient for a tracer particle in a suspension of equal hard spheres is expected to be $\tilde{a}_l(1,1) = 2.10$, see, e.g., Ref. 21. Our theory yields a slightly larger value $\tilde{a}_l(1,1) = 2.14$ since we neglect lubrication forces at small particle distances (which are less important if the interaction radius is larger than the hydrodynamic radius, i.e., for $\xi > 1$). For this reason $\tilde{a}_l$ for $\xi = 1$, while still being monotonic, shows the onset of a local maximum in our theory (see Fig. 3), which is in contrast to the results obtained in Refs. 5 and 37. For polymers with the same interaction radius as the tracer sphere we find $\tilde{a}_l(1, 1.6) = 0.66$. Therefore a tracer particle is much less hindered in its motion by a suspension of equal sized polymers than by a suspension of equal sized spheres. Because the polymer hydrodynamic radius is smaller than the hydrodynamic radius of the hard spheres, the tracer and the polymer interact less strongly via the solvent.

In order to test the accuracy of our results obtained with hydrodynamic tensors up to order $\mathcal{O}(r^{-11})$, we repeated the calculation with hydrodynamic tensors of the next lower order ($\mathcal{O}(r^{-9})$). The relative deviation Δ of the two results is $\Delta < 8\%$ ($\xi = 1$), $\Delta < 4\%$ ($\xi = 1.25$), $\Delta < 2\%$ ($\xi = 1.6$), and $\Delta < 1.1\%$ ($\xi = 2$) for both long and short time results. Δ vanishes for both $\zeta \rightarrow 0$ and $\zeta \rightarrow \infty$. As expected, the order of the expansion is less critical for $\xi > 1$, i.e., for small R_h, and taking into account even higher orders should not change the results for $\tilde{a}_{l/s}$ significantly. Calculations with lower order approximations to the diffusion tensors [$\mathcal{O}(r^{-7})$ or less] do not yield the correct generalized Stokes–Einstein relation, Eq. (28).

V. COMPARISON WITH EXPERIMENTS

A. Stretched exponential and scaling exponents

Experimental values of the long time diffusion coefficient (in the experimental papers, short and long time diffusion coefficients are not distinguished and we assume the long time value is measured) of tracer spheres in polymer solutions are often described empirically by a stretched exponential

$$\frac{D_s^l}{D_s^0} = e^{-C c^\nu M^\gamma R_s^\delta},\qquad(31)$$

with a dimensional constant C. It has been noticed that the form (31) has unphysical limits for both $\delta < 0$ and $\delta > 0$ for $R_s \rightarrow \infty$ and $R_s \rightarrow 0$ because one expects a finite value $D_s^l/D_s^0 \neq 1$ for any R_s. Rescaled versions have been suggested,[25,29] where only the difference between the limits

TABLE I. The exponents from Eq. (31) as measured in experiments compared to our theoretical prediction given by Eq. (33).

$R_g \lesssim R_s$	ν	γ	δ
Experiment[a]	$0.6,\dots,1.0$	0.8 ± 0.1	$-0.1,\dots,0.0$
Equation (33)	1	0.76	Weak dependence
$R_g \gtrsim R_s$			
Experiment[b]	$0.5,\dots,1.0$	$\cdots$	$0.69,\dots,1.0$
Equation (33)	1	0.76	$\delta>0$

[a]Reference 9.
[b]Reference 27.

$R_s \to \infty$ and $R_s \to 0$ is described by a stretched exponential. This rescaling makes a direct comparison of δ with experiments difficult, since experimental values are usually extracted from unrescaled data. Apart from this, the general experimental findings for the protein limit ($\zeta \gg 1$) are $\delta>0$ (see Ref. 27, Table I), i.e., D_s^l/D_s^0 decreases with R_s. In the colloid limit ($\zeta \ll 1$), D_s^l/D_s^0 was found to be almost independent of R_s with a negative $\delta \approx -0.1$.[9] The maximum of $\tilde{a}_l$ at $\zeta \approx 1$ (see Fig. 4) is therefore in qualitative agreement with experimental findings. Since $\tilde{a}_l$ is nonmonotonic as a function of ζ in our calculation, we conclude that D_s^l/D_s^0 cannot be described by a stretched exponential in R_s over the whole range of size ratios. This is in disagreement with Ref. 29, in which a universal value $\delta=0.77$ and a monotonic behavior was found. This difference might be due to the fact that our prediction is valid in the dilute limit, while the model in Ref. 29 is based on a depletion layer which is more pronounced at higher densities. We also emphasize that the *short time* diffusion coefficient decreases monotonically with R_s. In Ref. 29, the distortion of P which gives rise to the difference between short and long time diffusions was not taken into account.

Let us turn to the other exponents in Eq. (31). In the dilute limit, i.e., for small $c=\rho M/N_A$, the exponent in Eq. (31) is small and $D_s^l/D_s^0 \approx 1$. In this limit, for which our model is made, we get

$$\frac{D_s^l}{D_s^0} = 1 - Cc^\nu M^\gamma R_s^\delta + \mathcal{O}\{(Cc^\nu M^\gamma R_s^\delta)^2\}. \tag{32}$$

In terms of mass density c, our result for the long term diffusion constant in Eq. (25) reads

$$\frac{D_s^l}{D_s^0} = 1 - \frac{4\pi}{3}\tilde{a}_l R_g^3 c \frac{N_A}{M}. \tag{33}$$

As illustrated in Fig. 4, the dependence of $\tilde{a}_l$ on ζ, i.e., on the ratio of the polymer radius of gyration to the size of the tracer particle, is rather weak. We therefore neglect this dependence. Using the scaling of the polymer size with its mass, $R_g \propto M^{\nu_g}$,[38] we find by comparing Eqs. (32) and (33)

$$\gamma = 3\nu_g - 1. \tag{34}$$

In a good solvent, self-avoiding walk statistics for a Gaussian chain lead to $\nu_g=0.588$ for the average size of the polymer.[38] Using this value, we find
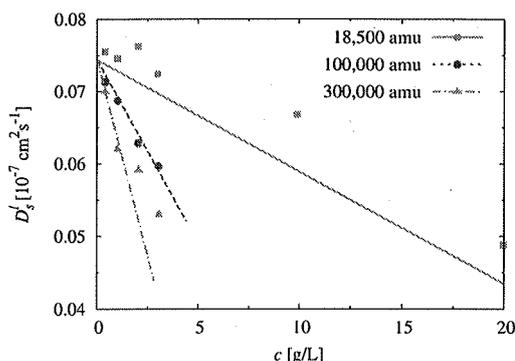

FIG. 5. Diffusion coefficient D_s^l of a polystyrene sphere of radius R_s $=322$ nm in a solution of PEO polymers with molecular masses of 18 500 amu (squares), 10^5 amu (circles), and 3×10^5 amu (triangles) from Ref. 8. The solid, dashed, and dashed-dotted lines, respectively, indicate the theoretical predictions for D_s^l according to Eq. (25). There is no adjustable parameter.

$$\gamma = 0.76, \tag{35}$$

with good agreement to the experimental value $\gamma=0.8$ found in Ref. 9. Note that the generalized Stokes–Einstein relation also leads to the expression in Eq. (34) for γ. The exponent ν of the concentration c is in our linear theory equal to unity by construction. In summary, all exponents compare well to the experimental findings, see Table I. For polymers at Θ-conditions with $\nu_g=0.5$ we predict $\gamma=0.5$.

The phenomenological law (31) is best valid at semidilute polymer concentrations as stated in Ref. 9. It is in fact nonanalytic in c for $\nu \neq 1$. Despite this, the experimental data summarized in Ref. 9 also cover the dilute regime and show similar behavior there, see Sec. V B. However, we found only very few experiments[10] focusing on the dilute regime.

B. Quantitative comparison

Our model does neither include long ranged forces between the tracer particle and the polymer coils nor adsorption of the polymer on the tracer. This situation is realized in
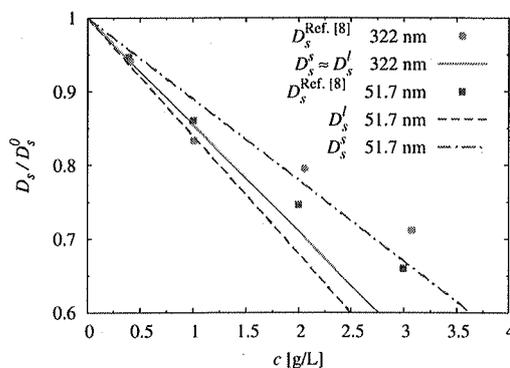

FIG. 6. Normalized diffusion coefficients D_s of spheres with radius R_s $=322$ and 51.7 nm (circle and square, respectively) in a solution of PEO with a molecular mass of 3×10^5 amu from Ref. 8. Dashed and dashed-dotted lines are theoretical predictions for D_s^l and D_s^s for $R_s=51.7$ nm in first order in polymer concentration from Eqs. (25) and (21), respectively. For $R_s=322$ nm, D_s^l and D_s^s are almost identical (corresponding to $\zeta=0.1$, see Fig. 4) and we only plot D_s^l (solid line).

Ref. 8: poly(ethylene oxide) (PEO) is a neutral polymer, so electrostatic interactions between the sphere and the polymers are absent, and polymer adsorption on the sphere is suppressed by a surfactant.

Neither the radius of gyration R_g nor the hydrodynamic radius R_h of the PEO polymers was measured in the experiments and we calculate them according to Ref. 39 via

$$R_g = 0.0215 M^{0.583} \text{ nm}, \tag{36}$$

$$R_h = 0.0145 M^{0.571} \text{ nm}. \tag{37}$$

Figure 5 compares the diffusion constants measured by light scattering [Ref. 8, Fig. 3(c)] with our results, which are by construction linear in the polymer mass density c. The tracer sphere (polystyrene) has a radius of $R_s = 322$ nm and the polymers have molecular masses of 18 500, 10^5, and 3 $\times 10^5$ amu. The experimental data for the smallest polymer with $M = 7500$ amu in [Ref. 8, Fig. 3(c)] were not useful at small concentrations due to large scatter. According to Ref. 8 the diffusion constant of the tracer particle in the pure solvent was $D_s^0 = 7.44 \times 10^{-9}$ cm^2 s^{-1}. Given these values, there is no fit parameter for the initial slopes in Fig. 5. The overlap concentration $c^* = 3M/(4\pi R_g^3 N_A)$ is 25.5, 7.1, and 3.2 g/L for the three polymers, respectively. Our theory, which is linear in the polymer concentration, is valid only for $c \ll c^*$. In Fig. 5, the experimental points start to deviate from the straight line for smaller and smaller c as M increases. For $M = 3 \times 10^5$ amu, they deviate considerably for $c > 1$ g/L. The agreement for concentrations much smaller than c^* is good in all three cases. Note that according to our theory the short time diffusion constant D_s^s is almost identical to D_s^l since the polymer coils are small as compared to the tracer particle, i.e., $\zeta \ll 1$, for the cases shown.

Figure 6 shows the normalized diffusion coefficient for two different sphere sizes [322 and 51.7 nm with $D_s^0 = 4.64 \times 10^{-8}$ cm^2 s^{-1} (Ref. 8)] in a solution with a polymer mass of 3×10^5 amu. For small polymer concentrations the normalized diffusion coefficient depends only weakly on the sphere size. For the smaller sphere, the ratio of R_g to R_s is given by $\zeta = 0.65$, such that a continuum theory is not expected to hold. For this value, long and short time coefficients should differ appreciably but the experimental values lie between our predictions for the short and long time diffusion constants. From Ref. 8 it is not clear weather the experiments probe the long or the short time coefficient. Note that at higher concentrations, the larger sphere is less hindered in the diffusion by the polymers, which is consistent with a negative value of δ.

VI. SUMMARY

We developed expressions for the short time and the long time diffusion coefficients of a tracer sphere in a dilute solution of particles with a hydrodynamic radius, which can be smaller than the hard-sphere radius for the interaction with the tracer particle, e.g., polymers. Solvent mediated hydrodynamic interactions are taken into account up to 11th order in reciprocal distance, therefore neglecting lubrication

forces at close distances. Calculating the diffusion coefficients is reduced to the solution of a system of 11 algebraic equations.

The results are in good agreement with experiments in the dilute regime, in which the diffusion constant depends in an affine way on the polymer density. While the short time diffusion coefficient decreases monotonically as a function of the size of the tracer particle, polymers with hydrodynamic radius comparable to the tracer size seem to be most efficient in decreasing the long time diffusion coefficient.

Our current model is limited to low polymer densities, but direct polymer-polymer interactions can be taken into account in the framework of a dynamic density functional theory.[12] Hydrodynamic interactions between the polymers and the tracer sphere can be taken into account in the same way as in this paper,[14] and recently dynamic density functional theory has been extended in order to take into account hydrodynamic interactions among the polymer coils.[40]

ACKNOWLEDGMENTS

APPENDIX: DIFFUSIVITY MATRIX

The coefficients $D_{ij}^\alpha(r)$, $\alpha \in \{r, \theta\}$, and $i,j \in \{s,p\}$ of the diffusivity matrix for a polymer (hydrodynamic radius R_h) and a spherical tracer particle of hydrodynamic radius R_s read up to order r^{-11} (Ref. 35),

$$D_{ss}^r(r) = 1 - \frac{15}{4} R_h^3 R_s \left(\frac{1}{r}\right)^4 + \left(\frac{15 R_h^3 R_s^3}{2} - 2 R_h^5 R_s\right)\left(\frac{1}{r}\right)^6$$

$$- \frac{3}{4} R_s(3 R_h^7 - 22 R_s^2 R_h^5 + 5 R_s^4 R_h^3)\left(\frac{1}{r}\right)^8$$

$$- \frac{1}{4} R_h^5 R_s(9 R_h^4 - 120 R_s^2 R_h^2 + 375 R_s^3 R_h + 70 R_s^4)$$

$$\times \left(\frac{1}{r}\right)^{10} + O\left(\left(\frac{1}{r}\right)^{12}\right), \tag{A1}$$

$$D_{ss}^\theta(r) = 1 - \frac{17}{16} R_h^5 R_s \left(\frac{1}{r}\right)^6 - \frac{1}{8} R_s(9 R_h^7 - 9 R_s^2 R_h^5 + 10 R_s^4 R_h^3)$$

$$\times \left(\frac{1}{r}\right)^8 - \frac{3}{16} R_s(6 R_h^9 - 18 R_s^2 R_h^7 + 35 R_s^4 R_h^5)\left(\frac{1}{r}\right)^{10}$$

$$+ O\left(\left(\frac{1}{r}\right)^{12}\right), \tag{A2}$$

$$D_{pp}^r(r) = 1 - \frac{15}{4}R_h R_s^3 \left(\frac{1}{r}\right)^4 + \left(\frac{15R_h^3 R_s^3}{2} - 2R_h R_s^5\right)\left(\frac{1}{r}\right)^6$$

$$- \frac{3}{4}R_h(3R_s^7 - 22R_h^2 R_s^5 + 5R_h^4 R_s^3)\left(\frac{1}{r}\right)^8$$

$$- \frac{1}{4}R_h R_s^5 (70R_h^4 + 375R_s R_h^3 - 120R_s^2 R_h^2 + 9R_s^4)$$

$$\times \left(\frac{1}{r}\right)^{10} + O\left(\left(\frac{1}{r}\right)^{12}\right), \tag{A3}$$

$$D_{pp}^\theta(r) = 1 - \frac{17}{16}R_h R_s^5 \left(\frac{1}{r}\right)^6 - \frac{1}{8}R_h(9R_s^7 - 9R_h^2 R_s^5 + 10R_h^4 R_s^3)$$

$$\times \left(\frac{1}{r}\right)^8 - \frac{3}{16}R_h(6R_s^9 - 18R_h^2 R_s^7 + 35R_h^4 R_s^5)\left(\frac{1}{r}\right)^{10}$$

$$+ O\left(\left(\frac{1}{r}\right)^{12}\right), \tag{A4}$$

$$D_{sp}^r(r) = \frac{3R_s}{2r} - \frac{1}{2}R_s(R_h^2 + R_s^2)\left(\frac{1}{r}\right)^3 + \frac{75}{4}R_h^3 R_s^4\left(\frac{1}{r}\right)^7$$

$$- \frac{15}{4}R_h^3 R_s^4(R_h^2 + R_s^2)\left(\frac{1}{r}\right)^9 + \frac{3}{4}R_s^4(10R_h^7$$

$$- 151R_s^2 R_h^5 + 10R_s^4 R_h^3)\left(\frac{1}{r}\right)^{11} + O\left(\left(\frac{1}{r}\right)^{13}\right), \tag{A5}$$

$$D_{sp}^\theta(r) = \frac{3R_s}{4r} + \frac{1}{4}R_s(R_h^2 + R_s^2)\left(\frac{1}{r}\right)^3 + \frac{7}{128}R_s^4(80R_h^7$$

$$- 79R_s^2 R_h^5 + 80R_s^4 R_h^3)\left(\frac{1}{r}\right)^{11} + O\left(\left(\frac{1}{r}\right)^{13}\right). \tag{A6}$$

[1] D. E. Dunstan and J. Stokes, Macromolecules 33, 193 (2000).
[2] W. Brown and R. Rymden, Macromolecules 21, 840 (1988).
[3] S. Harris, J. Phys. A 9, 1895 (1976).
[4] B. U. Felderhof, J. Phys. A 11, 929 (1978).
[5] G. K. Batchelor, J. Fluid Mech. 131, 155 (1983).

[6] M. Medina-Noyola, Phys. Rev. Lett. 60, 2705 (1988).
[7] D. S. Dean and A. Lefèvre, Phys. Rev. E 69, 061111 (2004).
[8] G. S. Ullmann, K. Ullmann, R. M. Lindner, and G. D. J. Phillies, J. Chem. Phys. 89, 692 (1985).
[9] G. D. J. Phillies, G. S. Ullmann, K. Ullmann, and T.-H. Lin, J. Chem. Phys. 82, 5242 (1985).
[10] G. D. J. Phillies, M. Lacroix, and J. Yambert, J. Chem. Phys. 101, 5124 (1997).
[11] G. D. J. Phillies, Biopolymers 24, 379 (1985).
[12] F. Penna, J. Dzubiella, and P. Tarazona, Phys. Rev. E 68, 061407 (2003).
[13] T. M. Squires and J. F. Brady, Phys. Fluids 17, 073101 (2005).
[14] M. Rauscher, A. Domínguez, M. Krüger, and F. Penna, J. Chem. Phys. 127, 244906 (2007).
[15] C. Gutsche, F. Kremer, M. Krüger, M. Rauscher, R. Weeber, and J. Harting, J. Chem. Phys. 129, 084902 (2008).
[16] J. Dzubiella, H. Löwen, and C. N. Likos, Phys. Rev. Lett. 91, 248301 (2003).
[17] M. Krüger and M. Rauscher, J. Chem. Phys. 127, 034905 (2007).
[18] D. Bedeaux and P. Mazur, Physica (Amsterdam) 76, 247 (1974).
[19] M. Pagitsas, J. T. Hynes, and R. Kapral, J. Chem. Phys. 71, 4492 (1979).
[20] R. I. Cukier, R. Kapral, J. R. Lebenhaft, and J. R. Mehaffey, J. Chem. Phys. 73, 5244 (1980).
[21] J. K. G. Dhont, An Introduction to Dynamics of Colloids (Elsevier, New York, 1996).
[22] A. G. Ogston, B. N. Preston, and J. D. Wells, Proc. R. Soc. London, Ser. A 333, 297 (1973).
[23] R. I. Cukier, Macromolecules 17, 252 (1984).
[24] A. R. Altenberger and M. Tirrell, J. Chem. Phys. 80, 2208 (1984).
[25] D. Langevin and F. Rondelez, Polymer 19, 875 (1978).
[26] L. Masaro and X. X. Zhu, Prog. Polym. Sci. 24, 731 (1999).
[27] T. Odijk, Biophys. J. 79, 2314 (2000).
[28] R. Tuinier, J. K. G. Dhont, and T.-H. Fan, Europhys. Lett. 75, 929 (2006).
[29] R. Tuinier and T.-H. Fan, Soft Matter 4, 254 (2008).
[30] G. K. Batchelor, J. Fluid Mech. 52, 245 (1972).
[31] B. U. Felderhof and R. B. Jones, Faraday Discuss. Chem. Soc. 76, 179 (1983).
[32] S. Hanna, W. Hess, and R. Klein, Physica A 111, 181 (1982).
[33] H. Zhang and G. Nägele, J. Chem. Phys. 117, 5908 (2002).
[34] B. Cichocki and B. U. Felderhof, J. Chem. Phys. 94, 556 (1991).
[35] D. J. Jeffrey and Y. Onishi, J. Fluid Mech. 139, 261 (1984).
[36] B. Dünweg, D. Reith, M. Steinhauser, and K. Kremer, J. Chem. Phys. 117, 914 (2002).
[37] G. Nägele, J. Phys.: Condens. Matter 15, S407 (2003).
[38] M. Doi and S. F. Edwards, The Theory of Polymer Dynamics (Clarendon Press, Oxford, 1986).
[39] K. Devanand and J. C. Selser, Macromolecules 24, 5943 (1991).
[40] M. Rex and H. Löwen, Phys. Rev. Lett. 101, 148302 (2008).